



Supporting Information

for

Atomic layer deposited films of Al₂O₃ on fluorine-doped tin oxide electrodes: stability and barrier properties

Hana Krýsová, Michael Neumann-Spallart, Hana Tarábková, Pavel Janda,
Ladislav Kavan and Josef Krýsa

Beilstein J. Nanotechnol. **2021**, *12*, 24–34. [doi:10.3762/bjnano.12.2](https://doi.org/10.3762/bjnano.12.2)

Additional figures

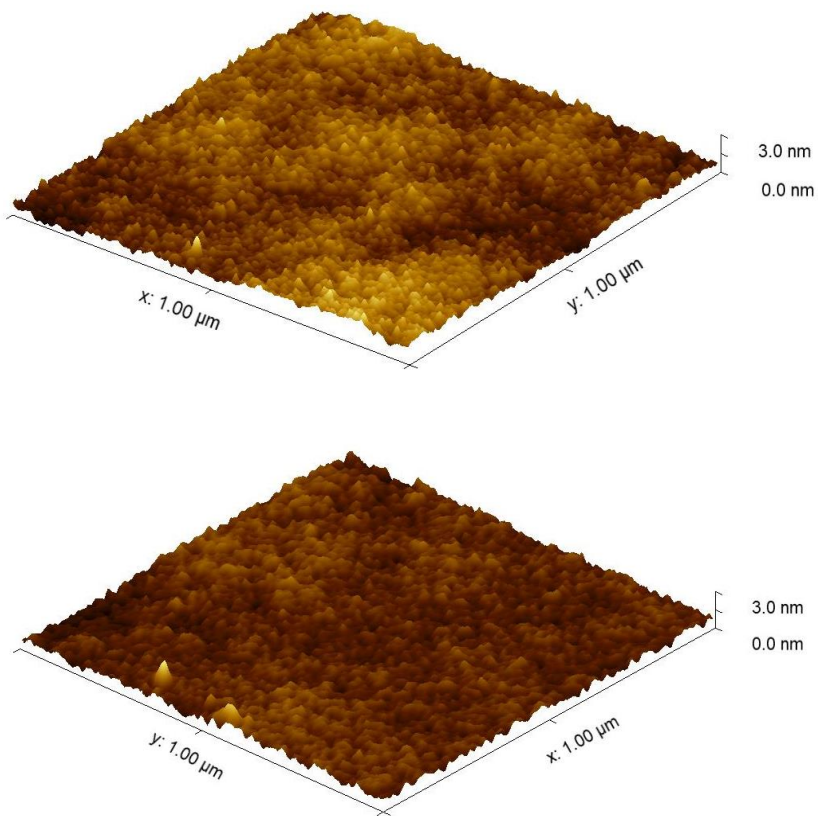


Figure S1: AFM surface morphology of Si/SiO₂ (bottom) and Si/SiO₂ coated with 17 nm Al₂O₃ (top).

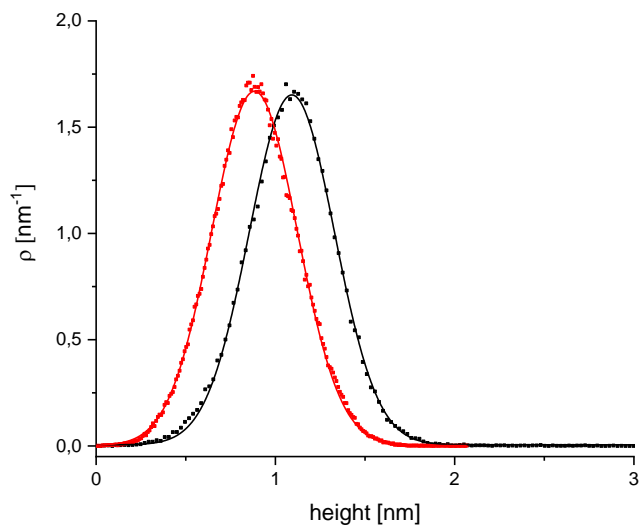


Figure S2: Height-density distribution calculated from AFM topography images (1 μm × 1 μm) of Si/SiO₂ (black dots) and Si/SiO₂ coated with 17 nm Al₂O₃ (red dots).

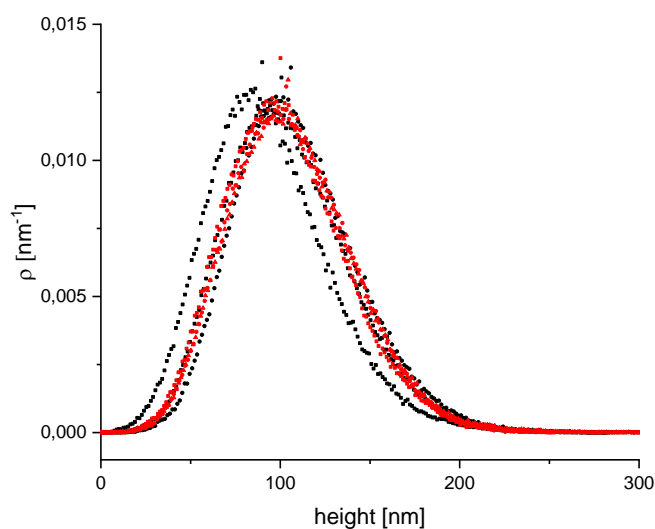


Figure S3: Height-density distribution calculated from AFM topography images ($10 \mu\text{m} \times 10 \mu\text{m}$) of three locations on the FTO substrate (black dots) and on FTO coated by 17 nm Al_2O_3 (red dots).

The effective pinhole area (EPA), defined as a ratio of A_u to A_0 , can be expressed as ratio of j_p to $j_{p,\text{FTO}}$, where j_p is the peak current density (with reference to the projected electrode area, A_0) measured at the actual blocking electrode. A_u is the uncovered area of FTO and $j_{p,\text{FTO}}$ is the current density peak measured at a bare FTO electrode. As suggested in previous works [1,2], there are two types of defects in the barrier film: i) The “defect A”, in which the partially blocked electrode behaves like “clean” FTO but with a relatively smaller effective area. The relative increase of the voltammetric peak separation (ΔE_{pp}) on the blocking layer normalized to that of pure FTO is smaller than three (ΔE_{pp} is defined as the difference between the peak potential values for the $\text{Fe}(\text{CN})_6^{4-}$ oxidation and $\text{Fe}(\text{CN})_6^{3-}$ reduction). ii) The “defect B” is a more complex situation, in which the defect not only causes the delamination of the titania film from the FTO substrate, but also the slowdown of charge transfer kinetics (accompanied by a strong increase in ΔE_{pp}).

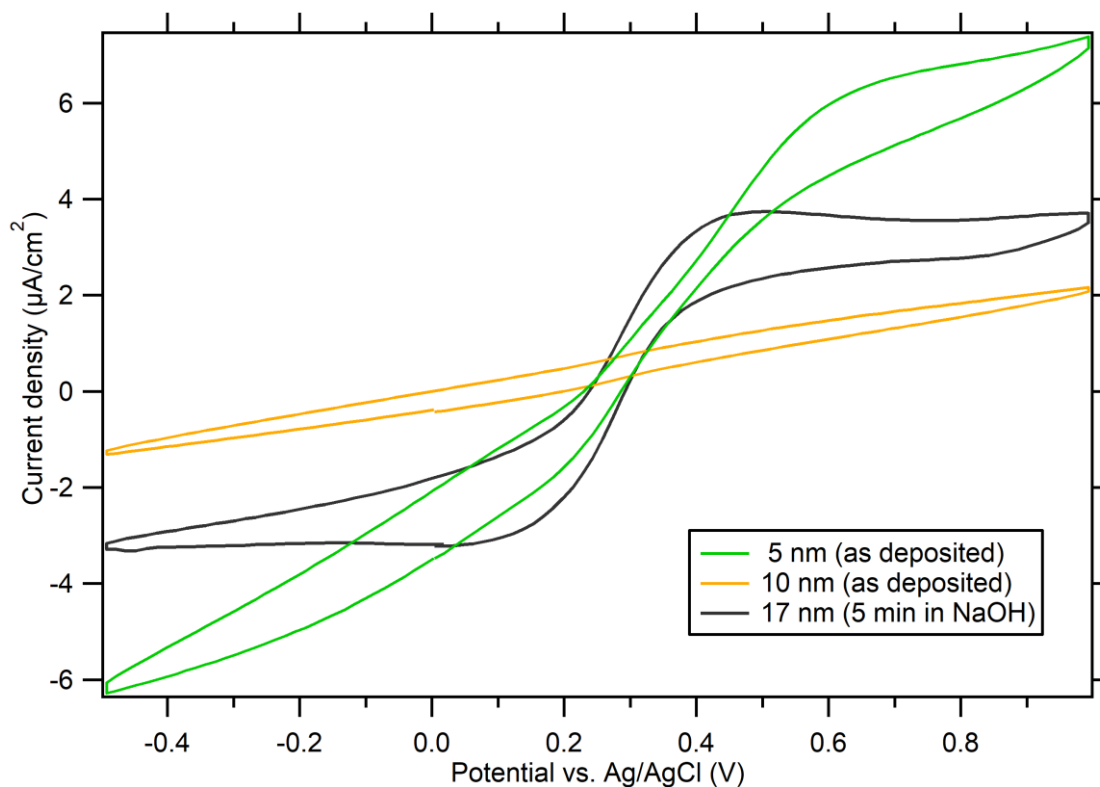


Figure S4: CVs of 0.5 mM $\text{K}_3[\text{Fe}(\text{CN})_6]$ and 0.5 mM $\text{K}_4[\text{Fe}(\text{CN})_6]$ in 0.5 M KCl, demonstrating the blocking properties of 5 and 10 nm Al_2O_3 films on FTO electrodes compared to 17 nm Al_2O_3 films on FTO, after an exposure to 1 M NaOH for 5 min. The scan rate is 50 mV/s.

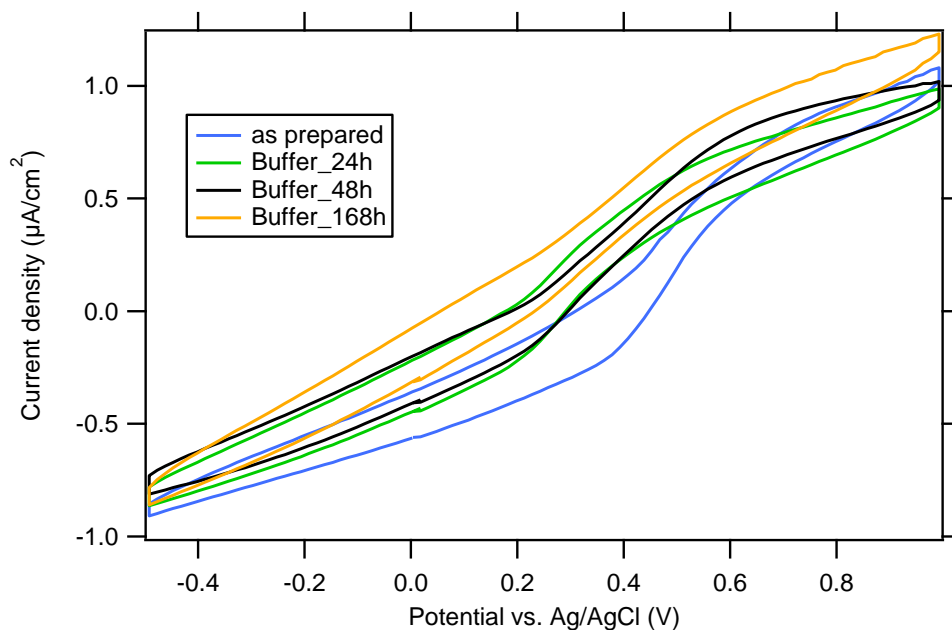


Figure S5: Details of the blocking properties of 17 nm Al_2O_3 films before and after exposure to phosphate buffer (pH 7.2) for 24, 48, and 168 hours. Cycling voltammetry in the presence of 0.5 mM $\text{K}_3[\text{Fe}(\text{CN})_6]$ and 0.5 mM $\text{K}_4[\text{Fe}(\text{CN})_6]$ in 0.5 M KCl. The scan rate is 50 mV/s.

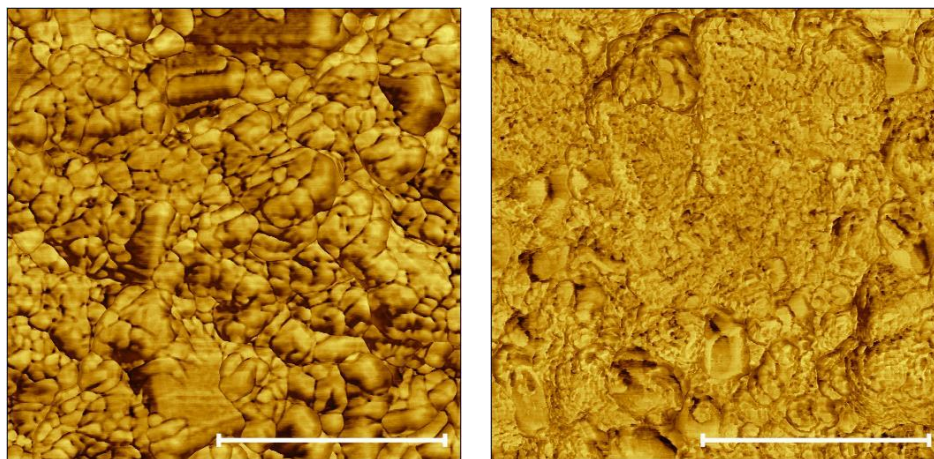


Figure S6: AFM phase image ($1 \mu\text{m} \times 1 \mu\text{m}$) of an FTO substrate before (left) and after (right) electrochemical treatment (-1.2 V, 5 h, phosphate buffer pH 7.2). White bars represent 500 nm.

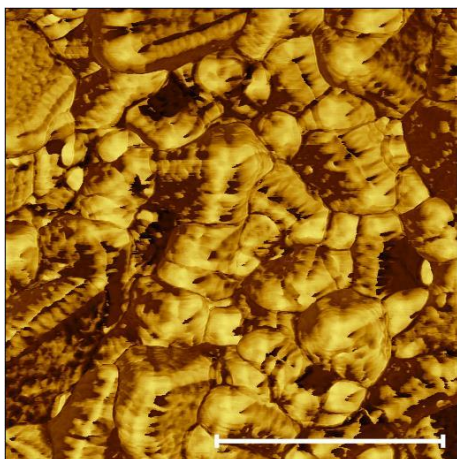


Figure S7: AFM phase image ($1\ \mu\text{m} \times 1\ \mu\text{m}$) of FTO substrate with 10 nm Al_2O_3 film after electrochemical treatment ($-1.2\ \text{V}$, 5 h, phosphate buffer, pH 7.2). The white bar represents 500 nm.

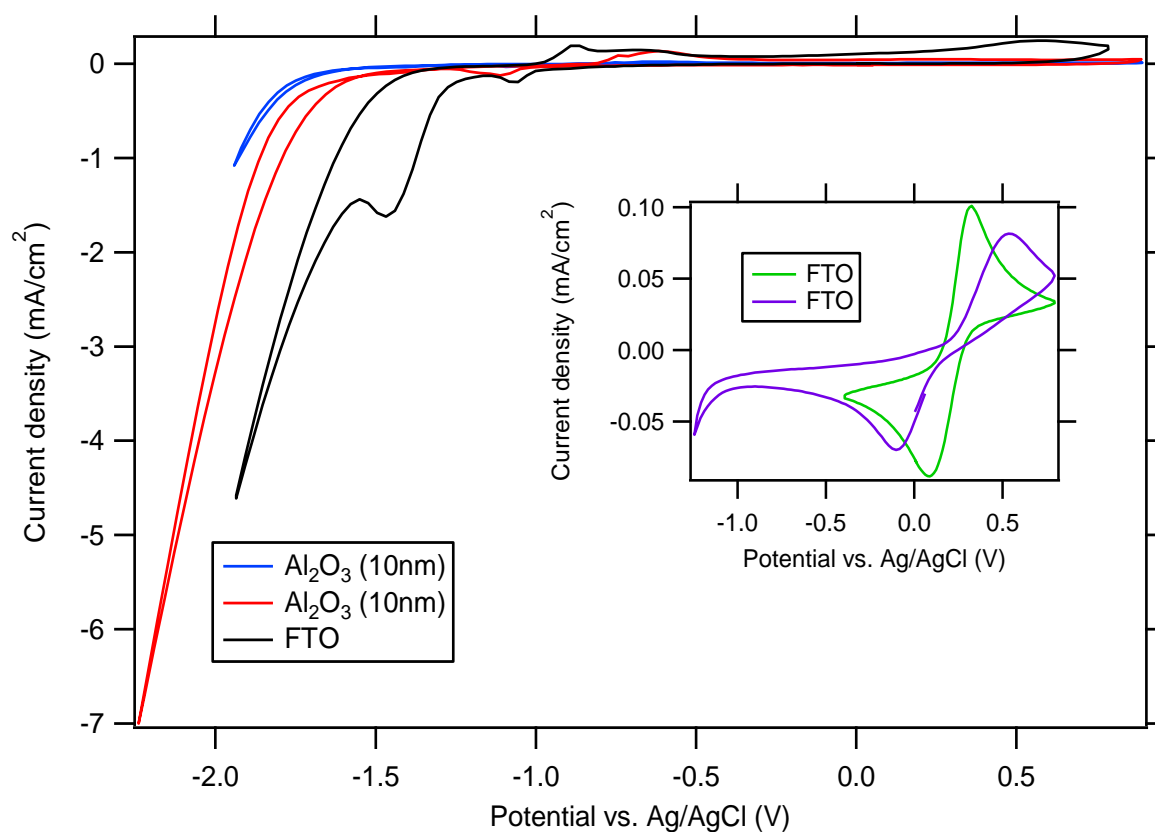


Figure S8: Cyclic voltammograms of $0.5\ \text{mM}\ \text{K}_3[\text{Fe}(\text{CN})_6]$ and $0.5\ \text{mM}\ \text{K}_4[\text{Fe}(\text{CN})_6]$ in phosphate buffer solution (pH 7.2) demonstrating a cathodic breakdown of FTO and its stabilization by coating with a 10 nm Al_2O_3 film. Inset: details of voltammograms on blank FTO with two different cathodic vertex potentials. The scan rate is $50\ \text{mV}/\text{s}$.

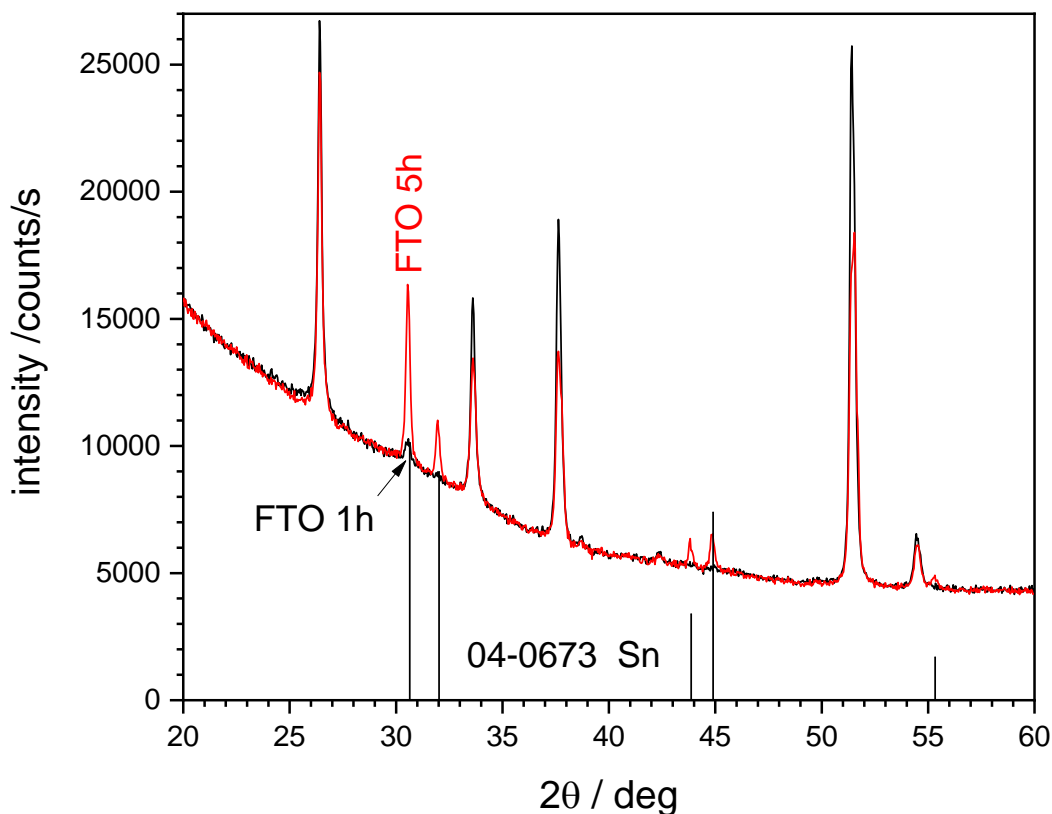


Figure S9: XRD patterns of unprotected FTO layers polarized at -1.2 V vs Ag/AgCl in buffer (pH 7.2) for 1 and 5 h. The Sn pattern was obtained from [3].

References

1. Kavan, L.; Tétreault, N.; Moehl, T.; Grätzel, M. *J. Phys. Chem. C* **2014**, *118*, 16408–16418. doi:[10.1021/jp4103614](https://doi.org/10.1021/jp4103614)
2. Krýsová, H.; Krýsa, J.; Kavan, L. *Beilstein J. Nanotechnol.* **2018**, *9*, 1135–1145. doi:[10.3762/bjnano.9.105](https://doi.org/10.3762/bjnano.9.105)
3. Powder Diffraction File Alphabetic PDF-2 Data Base, International Center of Diffraction Data, Newtown Square, PA, USA, 1994.